

Impact of Subsurface Temperature Variability on Meteorological Variability: An AGCM Study

Sarith P.P. Mahanama^{*†} Randal D. Koster[†] Rolf H. Reichle^{*†}

Max J. Suarez[†]

February 9, 2007

*Goddard Earth Sciences and Technology Center,
University of Maryland, Baltimore County,
Baltimore, MD 21250, USA.

†NASA Goddard Space Flight Center,
Code 610.1, Global Modeling and Assimilation Office,
Greenbelt, MD 20771, USA.

Corresponding author address:

Sarith Mahanama,
NASA Goddard Space Flight Center,
Code 610.1, Global Modeling and Assimilation Office,
Greenbelt, MD 20771, USA.

Email: sarith@gmao.gsfc.nasa.gov

Tel: (+1) 301-614-5667, FAX: (+1) 301-614-6297

submitted to the *Journal of Hydrometeorology*

Abstract

Anomalous atmospheric conditions can lead to surface temperature anomalies, which in turn can lead to temperature anomalies deep in the soil. The deep soil temperature (and the associated ground heat content) has significant memory – the dissipation of a temperature anomaly may take weeks to months – and thus deep soil temperature may contribute to the low frequency variability of energy and water variables elsewhere in the system. The memory may even provide some skill to subseasonal and seasonal forecasts.

This study uses three long-term AGCM experiments to isolate the contribution of deep soil temperature variability to variability elsewhere in the climate system. The first experiment consists of a standard ensemble of AMIP-type simulations, simulations in which the deep soil temperature variable is allowed to interact with the rest of the system. In the second experiment, the coupling of the deep soil temperature to the rest of the climate system is disabled – at each grid cell, the local climatological seasonal cycle of deep soil temperature (as determined from the first experiment) is prescribed. Finally, a climatological seasonal cycle of sea surface temperature (SST) was prescribed in the third experiment. Together, the three experiments allow us to isolate the contributions of variable SSTs, interactive deep soil temperature, and chaotic atmospheric dynamics to meteorological variability.

The results show that allowing an interactive deep soil temperature does indeed significantly increase surface air temperature variability. An interactive deep soil temperature, however, reduces the variability of the hydrological cycle (evaporation and precipitation), largely because it allows for a negative feedback between evaporation and temperature.

Contents

1	Introduction	5
2	Experiment Description	7
2.1	Models Used	7
2.2	Simulations Performed	9
3	Overall Evaluation of AGCM simulations	10
4	Results	12
4.1	Variability of Near-Surface Air Temperature	12
4.2	Connection to the Hydrological Cycle	15
5	Summary and Discussion	18
	References	20

1 Introduction

An anomalous atmospheric event – heavy rains, for example, spanning several days or a reduced monthly solar radiation due to persistent cloudiness – can induce substantial anomalies in moisture and energy reservoirs below the land surface. Depending on the nature of the various physical processes underlying moisture and heat transfer, dissipation of such anomalies may take weeks to months. Anomalies with such timescales are of critical importance to subseasonal and seasonal prediction, for it is through such anomalies and their links to atmospheric processes that predictive skill is realized.

The lifetime of land surface anomalies is shorter than that of ocean anomalies. Largely because of this, studies of land moisture impacts on forecasts [e.g. Delworth and Manabe (1988), Fennessy and Shukla, 1999, Liu and Avissar (1999)^{a,b}, Dirmeyer, (2000), Douville (2003), Mahanama and Koster (2003), Koster et al. (2004)] have lagged behind those of ocean impacts [e.g. Kumar and Hoerling (1995) and Shukla (1998)], and the initialization of the land surface in operational seasonal forecast systems is considered much less important than ocean initialization. Even so, land moisture initialization is beginning to receive more attention, particularly given its potential importance in regions and seasons for which the ocean has little impact [Koster et al. (2000)].

While studies of land moisture variability and its effects on climate are still somewhat immature, they are much farther along than corresponding studies of the climatic impacts of changes in heat content. Only a few published studies have addressed the latter problem. For example, Xue et al. (2002) demonstrated in a modeling study that deep soil temperatures over the western United States (US) in

late spring have an impact on US summer precipitation. Hu and Feng (2004)^{a,b} analyzed deep soil data from about 300 stations in the contiguous United States covering 30 years and found timescales for soil temperature anomalies of about 2-3 months. They also found evidence of a connection between the late spring temperature and summer precipitation. After analyzing observed soil moisture data and simulated soil temperature data, Amenu et al. (2005) concluded that the persistence of soil moisture at all soil layers is almost twice that of soil temperature.

In the present paper, we undertake to investigate further the impact of land heat content variations on climate variability in an Atmospheric General Circulation Model (AGCM). Our analysis focuses chiefly on two AGCM simulations: one in which the model's deep soil temperature was free to vary in response to variations in atmospheric forcing at the surface, and another in which the deep soil temperature at each grid cell was prescribed to a climatological seasonal cycle. In effect, variations in subsurface temperature were allowed to feed back on climate only in the first simulation. Isolating the impact of subsurface temperature variations on climate is the critical first step toward establishing the usefulness of its initialization for forecasts. A supplemental simulation with prescribed climatological SSTs was also examined to account for the impact of SST variability on meteorological variables (mainly, near-surface air temperature).

Section 2 provides a brief description of the AGCM and its component LSM (Land Surface Model). This section also describes the setup of the experiment. An evaluation of the AGCM's ability to represent observed surface and air temperature variability is provided in Section 3. Section 4 presents results illustrating the impact of deep soil temperature variability on above-ground climate variability.

2 Experiment Description

2.1 Models Used

The NSIPP-1 (NASA Seasonal-to-Interannual Project-1) forecasting system produced the simulations examined in this paper. The atmospheric component of the system has a finite-differenced, primitive equations dynamical core that allows arbitrary horizontal and vertical resolution. It uses a finite-difference C-grid, on latitude-longitude coordinates in the horizontal and a generalized sigma coordinate in the vertical (Suarez and Takacs, 1995). Model physics includes penetrative convection with the relaxed Arakawa–Schubert scheme (Moorthi and Suarez, 1992), Richardson number-dependent fluxes in the surface layer, and a sophisticated treatment of radiation, including the Chou and Suarez (1994) parameterization of longwave radiation and the calibration of the cloud parameterization scheme with Earth Radiation Budget Experiment (ERBE) and International Satellite Cloud Climatology Project (ISCCP) data.

The Mosaic LSM (Land Surface Model) (Koster and Suarez, 1992, 1996) constitutes the land component of the NSIPP-1 forecasting system. The Mosaic LSM separates each grid cell into subgrid "tiles" based on vegetation class and then performs separate energy and water balance calculations over each tile. Following the approach of Sellers et al. (1986), vegetation explicitly affects the balance calculations within a tile in several ways: (a) stomatal resistance increases during times of environmental stress, thereby reducing transpiration; (b) vegetation phenology helps determine the albedo and thus the net radiation; and (c) the "roughness" of the vegetation affects the transfers of both momentum and the turbulent fluxes. All

the tile diagnostic quantities are aggregated to grid cell averages prior to analysis.

Subsurface heat storage is represented by two state variables: the surface temperature and the deep soil temperature, associated with heat capacities of $7 \times 10^4 \text{ Jm}^{-2}\text{K}^{-1}$ and $4.74 \times 10^6 \text{ Jm}^{-2}\text{K}^{-1}$, respectively. Fluxes of heat between the two reservoirs are computed using a variant of the force-restore formulation of Deardorff, (1978). In essence, the flux, G_D , of heat from the surface reservoir to the deep soil reservoir at a given time step is computed with:

$$G_D = -\frac{\omega dc}{\sqrt{2}}(T_D - T_C), \quad (1)$$

where ω is the frequency of the diurnal temperature cycle, d is the depth over which a diurnal temperature wave is felt, c is the volumetric heat capacity, T_D is the deep soil temperature, and T_C is the surface temperature.

The higher heat capacity of the deep soil reservoir relative to the surface reservoir (by a factor of about 70) gives the deeper reservoir a greater inertia, resulting in lower frequency variations and a lagged response to surface forcing. Figure 1 illustrates this behavior at a representative point (located in the western United States). The curves in Figure 1a, which were extracted from the ALO experiment described in section 2.2 below, show single, concurrent annual cycles of simulated daily surface temperature and daily deep soil temperature. The deep soil temperature T_D is forced only by T_C , and thus it follows roughly the same seasonal cycle as T_C . The response of T_D to variations in T_C , however, is clearly muted and delayed. Figure 1b shows

the mean seasonal cycles of T_C and T_D , as computed from 20 years of simulation. On average at this point, T_D lags T_C by about 10 days. The global distribution of lag time (not shown) indicates that a 10 day lag is indeed typical for this model.

The force-restore approach is rather simple compared to the more detailed approaches used in many of today’s LSMs –approaches that include, for example, multiple soil temperature layers and heat diffusivities that vary with moisture content. The simple approach, however, is deemed adequate here for a first-order analysis of deep soil temperature effects.

2.2 Simulations Performed

Three separate AGCM experiments were used to analyze temperature variability in AGCMs (Table 1). First, an AGCM simulation with a fully interactive land surface model (the Mosaic LSM) allowed both SST variability (prescribed from observations) and land surface processes to influence the atmosphere (experiment ALO). A total of 700-years of AGCM data were produced for ALO by a 10-member ensemble of AGCM simulations, each simulation spanning about 70 years (1930–2000) on a $2^\circ \times 2.5^\circ$ (lat/lon) grid. The second experiment (ALOT) was designed to prevent deep soil temperature variability from affecting the atmosphere. Aside from its shorter duration (ALOT covered a single 60-yr period, from 1930–1989), this experiment differed from ALO in only one way: in ALOT, the deep soil temperature at each grid cell was reset once each day to the ALO climatological value for that day at that grid cell. Because the prescribed climatology was derived directly from ALO, experiments ALO and ALOT have identical climatological seasonal cycles of T_D , while T_D varies interannually only in ALO. (Note that in ALOT, the evolution

of T_D away from climatology over the 24 hours following its prescription each day is considered negligible.)

In the third experiment (AL), the SST variability was disabled by prescribing the climatological seasonal cycle of SST from Reynolds and Smith (1995). The deep soil temperature, though was allowed to interact with the climate system, as in ALO. Experiment AL consisted of a single 200-year simulation.

3 Overall Evaluation of AGCM simulations

Since the conclusions of this paper depend on the deep soil temperature variability simulated by an AGCM, we begin with an evaluation of the model’s ability to simulate surface and subsurface temperature. Unfortunately, for deep soil temperature, a direct global evaluation is impossible because multi-decadal deep soil temperature measurements are virtually non-existent. For deep soil temperature, we must rely on an indirect evaluation that focuses on simulated surface temperatures. It is, after all, only through changes in surface temperature that changes in deep soil temperature are realized – both in nature and in the model.

Earth observing satellites have been taking measurements relevant to surface skin temperature for decades. The International Satellite Cloud Climatology Project (ISCCP) has produced global clear-sky skin temperature fields using satellite observations since 1982. For near-surface air temperature (T_{air}), the Climate Monitoring System (CAMS) has generated a global gridded data set using station data for the period 1946–2003. We use these two data sets to evaluate the temperatures simulated in experiment ALO. The top left panel in Figure 2 shows the global distribution of annual mean land surface temperature from ISSCP, derived by aggregating the

30km 3-hourly ISCCP data over the 1986-1995 period to a $1^\circ \times 1^\circ$ (lat/lon) grid. The annual mean T_{air} from the CAMS data is shown in the top right panel. Corresponding maps for experiment ALO (for the period 1930–1989) are shown in the bottom row. (Again, the AGCM data were produced on a $2^\circ \times 2.5^\circ$ grid, a total of 700-years of simulations provided the statistics for the ALO ensemble). Though not perfect, the AGCM annual mean temperatures in the ALO ensemble are in reasonable agreement with both satellite-based estimates and CAMS data.

For an evaluation of the interannual variability, we compute the standard deviation of monthly temperatures for each calendar month. The average (over the year) of the standard deviation of interannual variation of monthly temperature is shown in Figure 3 – for the ISCCP skin temperature (top left), CAMS T_{air} (top right), ALO surface temperature (bottom left), and ALO near-surface air temperature (bottom right). The model captures the general increase in variabilities from low to high latitudes, but it has some notable deficiencies. The AGCM underestimates variability throughout the tropics. Also, the AGCM’s surface temperature variability in high-latitudes is lower than that of the ISCCP data, possibly due to problems with the simulation of snow. (On the other hand, the simulation of T_{air} variability in high latitudes appears more reasonable.) Note that the ISCCP data reflect cloud-free conditions, while the AGCM data and the CAMS data reflect both cloud-free and overcast conditions.

Another manifestation of temperature variability relevant to this paper is the “memory” of temperature, as measured by its one-month-lagged autocorrelation. The top rows of Figures 4 and 5 provide comparisons (for boreal summer [JJA] and winter [DJF], respectively), of observed and simulated (in ALO) one-month-lagged

autocorrelation of T_{air} . [Note that the global distribution of one-month-lagged autocorrelation of T_D in ALO (not shown) showed approximately two times that of T_{air} .] For both seasons, the model performs reasonably well, capturing the tropical/extratropical distinction in memory seen in the observations and generally reproducing the correct magnitudes of the autocorrelations. As with the simulation of standard deviation, though, the model has some distinct deficiencies. Simulated memory, for example, is too high in the Great Plains of North America during JJA, undoubtedly due to the hydrological land-atmosphere coupling in this model, which is known to be excessive (Guo et al., 2006). Across the globe, memory in the model generally appears to be biased slightly high.

4 Results

4.1 Variability of Near-Surface Air Temperature

The bottom panels of Figures 4 and 5 show the impact of prescribing the deep soil temperature on surface memory. The difference maps (lower right panels) show that in both seasons, prescribing the deep soil temperature to climatology substantially reduces the memory of T_{air} in the extratropics. In other words, the heat reservoir associated with the deep soil temperature clearly adds memory to the above-surface climate system. The much larger impact in boreal winter is probably associated with the control of the deep soil on the evolution, maintenance and ablation of snowpack.

We now take advantage of the design of the experiments to characterize the interannual variance of monthly-mean near-surface air temperature ($\sigma_{T-\text{air}}^2$) in terms of three separate controls: SST variability, chaotic atmospheric dynamics, and deep

soil temperature. To illustrate how these three controls affect $\sigma_{T-\text{air}}^2$, we follow the approach of Koster et al. (2000), who performed an analogous analysis of precipitation variance. The approach rests on the assumption of a linear framework for expanding $\sigma_{T-\text{air}}^2$ of the control (ALO) experiment:

$$\sigma_{T-\text{air},\text{ALO}}^2 = \sigma_{T-\text{air},\text{ALOT}}^2 [X_O + (1 - X_O)] \frac{\sigma_{T-\text{air},\text{ALO}}^2}{\sigma_{T-\text{air},\text{ALOT}}^2}. \quad (2)$$

This equation, of course, is a tautology. The right hand side of the equation, however, can be interpreted in terms of the three aforementioned controls, allowing us to illustrate their separate contributions to the total variance ($\sigma_{T-\text{air},\text{ALO}}^2$). We interpret the first term, $\sigma_{T-\text{air},\text{ALOT}}^2$, as the air temperature variance a climate system would achieve in the absence of deep soil temperature variability; this term is computed directly from the ALOT experiment. The terms X_O and $1 - X_O$ are the fractional contributions of oceanic and random atmospheric processes, respectively, to $\sigma_{T-\text{air},\text{ALOT}}^2$; in analogy to Koster et al. (2000), we compute:

$$X_O = \frac{\sigma_{T-\text{air},\text{ALO}}^2 - \sigma_{T-\text{air},\text{AL}}^2}{\sigma_{T-\text{air},\text{ALO}}^2}. \quad (3)$$

Finally, we interpret the term $\frac{\sigma_{T-\text{air},\text{ALO}}^2}{\sigma_{T-\text{air},\text{ALOT}}^2}$ as the amplification of the variance $\sigma_{T-\text{air},\text{ALOT}}^2$ through interactions of the climate system with the deep soil temperature.

Koster et al. (2000) verified that the linear framework assumption is reasonably valid for the analysis of precipitation variance. A corresponding verification for air

temperature variance is not possible here, since we lack a critical fourth simulation – one in which climatologies of both SSTs and deep soil temperatures are specified (Apart from the ensemble ALOT, we used pre-existing AGCM simulations for the other two ensembles for our analysis. Computational time constraints did not permit another AGCM simulation in which climatologies of both SSTs and T_D were prescribed). We proceed, then, on the unproven assumption of linearity, pointing to its validity for precipitation and to the idea that temperature statistics are more likely to be well-behaved than precipitation statistics.

Thus, with this caveat, Figure 6 shows maps of all four terms for the boreal summer months and thus provides a full characterization of oceanic, atmospheric, and land contributions to near-surface air temperature variance. The upper left plot shows $\sigma_{T-\text{air},\text{ALOT}}^2$. Even in the absence of deep soil temperature interaction, the air temperature variance is much larger in midlatitudes than in the tropics. The very high values in the midwestern United States are associated with strong precipitation and evaporation variances there, and the occasional high value in polar latitudes may be related to interannual variations in late-season snow cover.

The upper right and lower left panels of Figure 6 show X_O and $1 - X_O$, the relative contributions of ocean variability and chaotic atmospheric dynamics to the air temperature variance. The oceanic contribution dominates only in the tropics. It is lower (of order 10-30%) in the subtropics and is close to zero throughout much of midlatitudes. Clearly, in this model, chaotic atmospheric dynamics has the largest impact on the interannual variability of near-surface air temperature over most of the globe. Perfect predictions of SSTs would not provide much skill in predicting midlatitude air temperature over continents.

The lower right panel of Figure 6 shows the amplification factor, $\frac{\sigma_{T-\text{air,ALO}}^2}{\sigma_{T-\text{air,ALOT}}^2}$. The interaction of the deep soil temperature with the climate system increases the air temperature variance significantly in most areas, with increases of 50% or more in the Sahara and in parts of western North America, southeastern South America, central Asia, and northern Australia. Increases are small or non-existent, however, throughout most of the tropics and in many high latitude areas.

Figure 7 shows the four corresponding plots for boreal winter. Variances produced in the absence of deep soil temperature interaction (upper left panel) appear to have increased almost everywhere in the northern hemisphere. Many of the higher values at higher latitudes presumably result from interannual variations in snow cover. The relative contributions of ocean variability and chaotic atmospheric dynamics to the air temperature variance look similar to the values for boreal summer, though with a southward shift in the ocean's dominance in the tropics, and with a general reversal of the southwest-northeast ocean contribution pattern in North America.

The amplification of the air temperature variance due to deep soil temperature interactions (lower right panel) is particularly different during boreal winter. Deep soil temperature interaction increases $\sigma_{T-\text{air}}^2$ by more than 50% in most midlatitude regions and by more than 200% in parts of northern Asia. Significant amplification is even seen in the tropics.

4.2 Connection to the Hydrological Cycle

Figure 8a shows the change in the variance of evaporation obtained when the deep soil temperatures are prescribed to climatological values. The change is strong and

positive over the midwestern United States, in stark contrast to the corresponding and opposite change in the variance of surface temperature. The change in the variance of precipitation is also large and positive over the midwestern United States (Figure 8b), in direct response to the change in evaporation variance. Apparently, the removal of interaction between the deep soil temperature and the rest of the climate system, while decreasing the variance of surface air temperature (Figure 8c), has increased the hydrological variance. The explanation for this behavior may lie in the negative feedback associated with the evaporative cooling of the land surface. In ALO, when a precipitation event causes a positive soil moisture anomaly, the evaporation following the event is anomalously large; this tends to cool the surface, and the evaporation anomaly, while still positive, is reduced. In ALOT, on the other hand, when the evaporation anomaly cools the surface, the prescribed deep soil temperature – effectively an infinite source of energy – helps to restore the surface temperature to its earlier, warmer state. The negative feedback is reduced, and the evaporation anomaly can remain large. This has the effect of increasing the average size of the anomaly and its associated variance.

The increase of evaporation variability in Figure 8a is in some ways akin to a well known problem with climate simulations that use prescribed SSTs (e.g., Barsugli and Battisti, 1998). In a coupled atmosphere-ocean model (and, for that matter, in nature), a sudden change in atmospheric temperature over the ocean initially leads to an increased vertical temperature gradient and thus to increased fluxes, but the gradient – and the fluxes – are reduced again as the ocean surface temperature adjusts to the overlying air temperature. In essence, the ability of the atmospheric and ocean surface temperatures in a coupled system to move in tandem

(to a degree) keeps the variability of the surface fluxes in check. With prescribed SSTs, however, one end of the temperature gradient is anchored, and as a result, any variability of atmospheric temperature leads to an overestimation of the variance of heat transport from the ocean surface. This limitation of non-coupled systems provides a potentially broader explanation for the increased variability in evaporation seen for the ALOT ensemble in Figure 8: an artificially lowered variance of surface temperature (due to the fixing of T_D) in the presence of atmospheric variability can similarly lead to an overestimated variance of vertical atmospheric gradients and thus of the surface heat fluxes.

The effect of prescribed deep soil temperatures on the variance of evaporation has major implications for the interpretation of certain AGCM results. While most AGCMs use a zero heat flux boundary condition in the deep soil and thereby allow deep soil temperature to vary prognostically, interacting with the rest of the climate system, a handful of AGCM and mesoscale modeling systems do rely on prescribed climatological deep soil temperatures [Environmental Modeling Center, (2003), Dudhia et al, (2005), and a handful AGCMs among the AMIP models in Phillips, (1994)]. The prescription does prevent climate drift in the system and is therefore advantageous, for example, for use in weather forecast systems. Figure 8, however, illustrates a distinct disadvantage of the approach. Depending on the depth of prescribed deep soil temperatures, a modeling system may overestimate the degree of land-atmosphere feedback in the system. Evaporation, and thus precipitation, may respond too strongly to variations in soil moisture. Land-atmosphere interaction studies performed with such models thus have a distinct limitation.

5 Summary and Discussion

This paper provides an analysis of the impacts of deep soil temperature variance on near-surface air temperature variability in an AGCM. Through the joint analysis of three AGCM experiments, we show in Figures 6 and 7 how interactive deep soil temperatures amplify the air temperature variance induced originally from SST variations and chaotic atmospheric dynamics. Interactive deep soil temperatures have their largest impact outside of the tropics, and their impact is significantly larger in boreal winter than in boreal summer. (The analysis also shows that the influence of SSTs on near-surface air temperature variance is essentially limited to the tropics.) These results, along with those in Figures 4 and 5 showing the contribution of deep soil temperatures to near-surface air temperature memory, suggest that the realistic initialization of deep soil temperature in a forecast model may have a positive impact on the forecast model's skill.

The impact of deep soil temperature variability on the hydrological cycle (in particular, on boreal summer precipitation and evaporation) was also examined. In contrast to its impact on air temperature variance, the removal of deep soil temperature variability increased the variability of evaporation and, as a result, precipitation (Figure 8). This is explained by negative feedbacks in the free running model (ALO). Positive soil moisture anomalies increase evaporation, but evaporative cooling at the surface acts as a negative feedback that reduces this increase. In ALOT, however, the prescription of deep soil temperature reduces the effectiveness of this negative feedback. These results suggest that any AGCM that prescribes a climatology of deep soil temperature may have a reduced usefulness for land-atmosphere interaction studies.

To highlight the impacts of deep soil temperature variability on climate, prescribing the seasonal cycle of this temperature was a natural strategy. A related question, one with potentially profound implications for the modeling of the land surface in prediction systems, has to do with the choice of the heat capacities used for subsurface temperature states. A study of Figure 8a might suggest the hypothesis that an increase in a model’s subsurface heat capacity could give it greater “inertia”, causing the model to reduce the negative feedback associated with evaporative cooling – in effect, giving the model an enhanced evaporation variability and thus an enhanced hydrological coupling with the atmosphere. The enhanced inertia might also affect the air temperature variability, as suggested in Figures 4 through 7 – not to the extremes indicated in the figures, but in those directions. The connection between the treatment of subsurface heat content and the rest of the climate system is complex and is the subject of ongoing research using more sophisticated thermodynamic models.

Acknowledgments

This research work was supported by funding from the Earth Science Enterprise of NASA Headquarters. The NASA Center for Computational Sciences provided computational resources. Ping Liu was instrumental in submitting and processing the ensemble ALOT. Phil Pegion helped with insightful discussions during the experiment. Mike Fennessy of Center for Ocean-Land-Atmosphere studies provided the gridded CAMS station data.

References

- Amenu, G. G., P. Kumar, and Liang, X., 2005: Interannual Variability of Deep-Layer Hydrologic Memory and Mechanisms of Its Influence on Surface Energy Fluxes. *J. Climate*, **18**, 5024–5045.
- Barsugli, J. J., and D. S. Battisti, 1998: The basic effects of atmosphere-ocean thermal coupling on midlatitude variability. *J. Atm. Sci.*, **55**, 477-493.
- Chou, M.-D., and M. Suarez, 1994: An efficient thermal infrared radiation parameterization for use in general circulation models. NASA Tech. Memo. 104606, Vol. 3, 84 pp. [Available from NASA Center for Aerospace Information, 800 Elkridge Landing Rd., Linthicum Heights, MD 21090-2934.]
- Deardoff, J. W, 1978: Efficient prediction of ground surface temperature and moisture, with inclusion of a layer vegetation. *J. Geophys. Res.*, **83**, 1889–1903.
- Delworth, T. L., and S. Manabe, 1988: The influence of potential evaporation on the variabilities of simulated soil wetness and climate. *J. Climate*, **1**, 523–547.
- Dirmeyer, P. A., 2000: Using a global soil wetness dataset to improve seasonal climate

- simulation. *J. Climate*, **13**, 2900-2922.
- Douville, H., (2003): Assessing the influence of soil moisture on seasonal climate variability with AGCMs. *J. Hydrometeorol.*, **4**, 1044–1066.
- Dudhia, J., D. Gill, K. Manning, W. Wang, and C. Bruyere, 2005: PSU/NCAR Mesoscale Modeling System, Tutorial Class Notes and User’s Guide: MM5 Modeling System Version 3, available at <http://www.mmm.ucar.edu/mm5/documents/tutorial-v3-notes.html>
- Environmental Modeling Center, 2003: The GFS Atmospheric Model, NCEP Office Note 442, 14pp.
- Fennessy, M. J., and J. Shukla, 1999: Impact of initial soil wetness on seasonal atmospheric prediction. *J. Climate*, **12**, 3167–3180.
- Guo, Z., P. A. Dirmeyer, R. D. Koster, and co-authors, 2006: GLACE: The Global LandAtmosphere Coupling Experiment. Part II: Analysis. *J. Hydrometeorol.*, **7**, 611–625.
- Hu, Q., and S. Feng, 2004: A role of the soil enthalpy in land memory. *J. Climate*, **17**, 3633–3643.
- Hu, Q., and S. Feng, 2004: Why has the land memory changed? *J. Climate*, **17**, 3236–3243.
- Phillips, T. J., 1994: A Summary Documentatation of the AMIP Models, PCMDI Report No. 18, 328pp.
- Koster, R. D., and M. J. Suarez, 1992: Modeling the land surface boundary in climate models as a composite of independent vegetation stands. *J. Geophys. Res.*, **97**, 2697–2715.
- Koster, R. D., and M. J. Suarez, 1996: Energy and water balance calculations in the MOSAIC LSM. NASA Tech. Memo. 104606, Vol. 9, 60 pp.

- Koster, R. D., M. J. Suarez, and M. Heiser, 2000: Variance and predictability of precipitation at seasonal-to-interannual timescales. *J. Hydrometeor.*, **1**, 26–46.
- Koster, R. D., M. J. Suarez, P. Liu, U. Jambor, A. Berg, M. Kistler, R. H. Reichle, M. Rodell, and J. Famiglietti, 2004: Realistic initialization of land surface states: Impacts on subseasonal forecast skill. *J. Hydrometeor.*, **5**, 1049–1063.
- Kumar, A., and M. P. Hoerling, 1995: Prospects and limitations of seasonal atmospheric GCM predictions. *Bull. Amer. Meteor. Soc.*, **76**, 335–345.
- Liu, Y., and R. Avissar, 1999a: A study of persistence in the land-atmosphere system using a general circulation model and observations. *J. Climate*, **12**, 2139–2153.
- Liu, Y., and R. Avissar, 1999b: A study of persistence in the land-atmosphere system using a fourth order analytical model. *J. Climate*, **12**, 2154–2168.
- Mahanama, S. P. P., and R. D. Koster, 2003: Intercomparison of soil moisture memory in two land surface models. *J. Hydrometeor.*, **4**, 1134–1146.
- Moorthi, S., and M. J. Suarez, 1992: Relaxed Arakawa–Schubert: A parameterization of moist convection for general circulation models. *Mon. Wea. Rev.*, **120**, 978–1002.
- Reynolds, R. W., and , 1995: A high-resolution global sea surface temperature climatology. *J. Climate*, **8**, 1571–1583.
- Sellers, P. J., Y. Mintz, Y. C. Sud, and A. Dalcher, 1986: A simple biosphere model (SiB) for use within general circulation model. *J. Atmos. Sci.*, **43**, 505–531.
- Suarez, M. J., and L. L. Takacs, 1995: Documentation of the ARIES/GEOS dynamical core: Version 2. NASA Tech. Memo. 104606, Vol. 5, 45 pp.
- Shukla, J., 1998: Predictability in the midst of chaos: A scientific basis for climate forecasting. *Science*, **282**, 728–731.
- Xue Y., L. Yi, M. Ruml, and R. Vasic, 2002: Investigation of Deep Soil Temperature-

Atmosphere Interaction in North America, The Mississippi River Climate and Hydrology Conference, 82nd AMS Annual Meeting, New Orleans, LA.

Figure List

Figure 1: (a) Seasonal cycles of surface temperature (T_C – dotted line) and deep soil temperature (T_D – dark line) for the grid cell at 120W, 38N from ensemble ALO for a representative year. (b) Climatological seasonal cycles of surface temperature (T_C – dotted line) and deep soil temperature (T_D – dark line) for the grid cell at 120W, 38N from ensemble ALO over 20–years.

Figure 2: (top left) Annual mean clear–sky skin temperature calculated from the ISCCP (1986-1995) data, (top right) Annual mean T_{air} from CAMS data, (bottom left) Annual mean surface temperature from the ensemble ALO, and (bottom right) Annual mean T_{air} from the ensemble ALO. For the CAMS plot, whited–out areas indicate a lack of data. Units are [K].

Figure 3: Standard deviations of monthly: (top left) skin temperature calculated for the ISCCP (1986-1995) data, (top right) T_{air} from CAMS data, (bottom left) surface temperature from the ensemble ALO, and (bottom right) T_{air} from the ensemble ALO. For the CAMS plot, whited–out areas indicate a lack of data. Units are [K]

Figure 4: One-month-lagged autocorrelation of T_{air} (ρ) for boreal summer (JJA): (top left) from CAMS, (top right) from the ensemble ALO, (bottom left) from the ensemble ALOT. (bottom right) Differences ALO – ALOT. For the CAMS plot, whited–out areas indicate a lack of data.

Figure 5: Same as Figure 4, but for the winter (DJF).

Figure 6: Breakdown of the contributions of oceanic, atmospheric, and deep soil temperature variance to T_{air} variance, assuming a linear framework for the boreal summer (JJA). Top left: T_{air} variance from ALOT [K^2]. Top right: The

fraction of the Tair variance induced by variable SSTs [XO from Eq. 3]. Bottom left: The fraction of the Tair variance induced by chaotic atmospheric dynamics (1–XO). Bottom right: Amplification of variance due to deep soil temperature variance ($\frac{\sigma_{ALO}^2}{\sigma_{ALOT}^2}$ for Tair).

Figure 7: Same as Figure 6, but for the winter months (DJF).

Figure 8: ALO and ALOT Comparison (ALOT – ALO) : (a) Difference in variance (σ^2) of evaporation for boreal summer (JJA) [mm^2d^{-1}], (b) same but for precipitation [mm^2d^{-1}], and (c) same but for surface temperature [K^2].

List of Tables

Table 1: Summary of experiments performed.

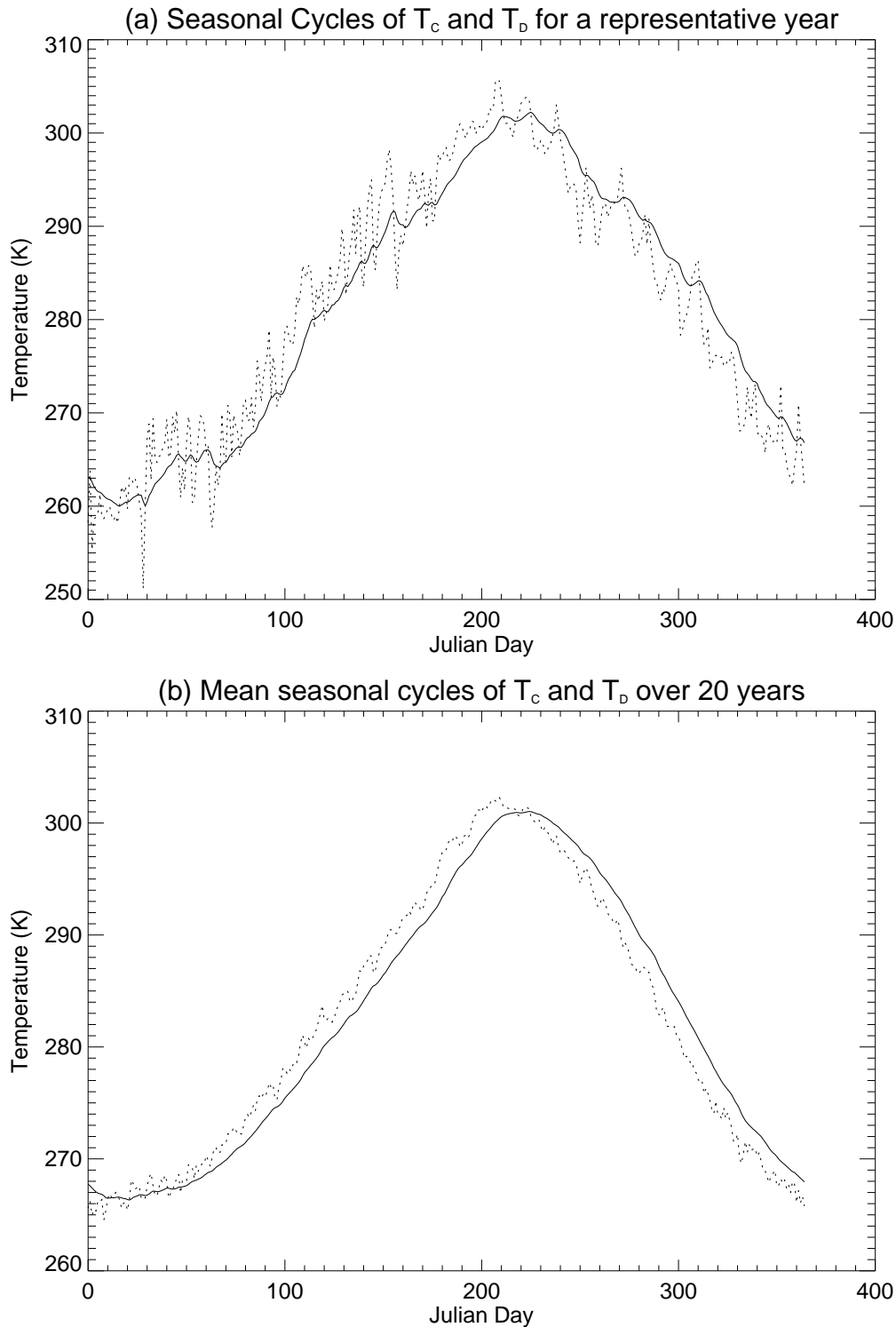


Figure 1: (a) Seasonal cycles of surface temperature (T_C – dotted line) and deep soil temperature (T_D – dark line) for the grid cell at 120W, 38N from ensemble ALO for a representative year. (b) Climatological seasonal cycles of surface temperature (T_C – dotted line) and deep soil temperature (T_D – dark line) for the grid cell at 120W, 38N from ensemble ALO over 20–years.

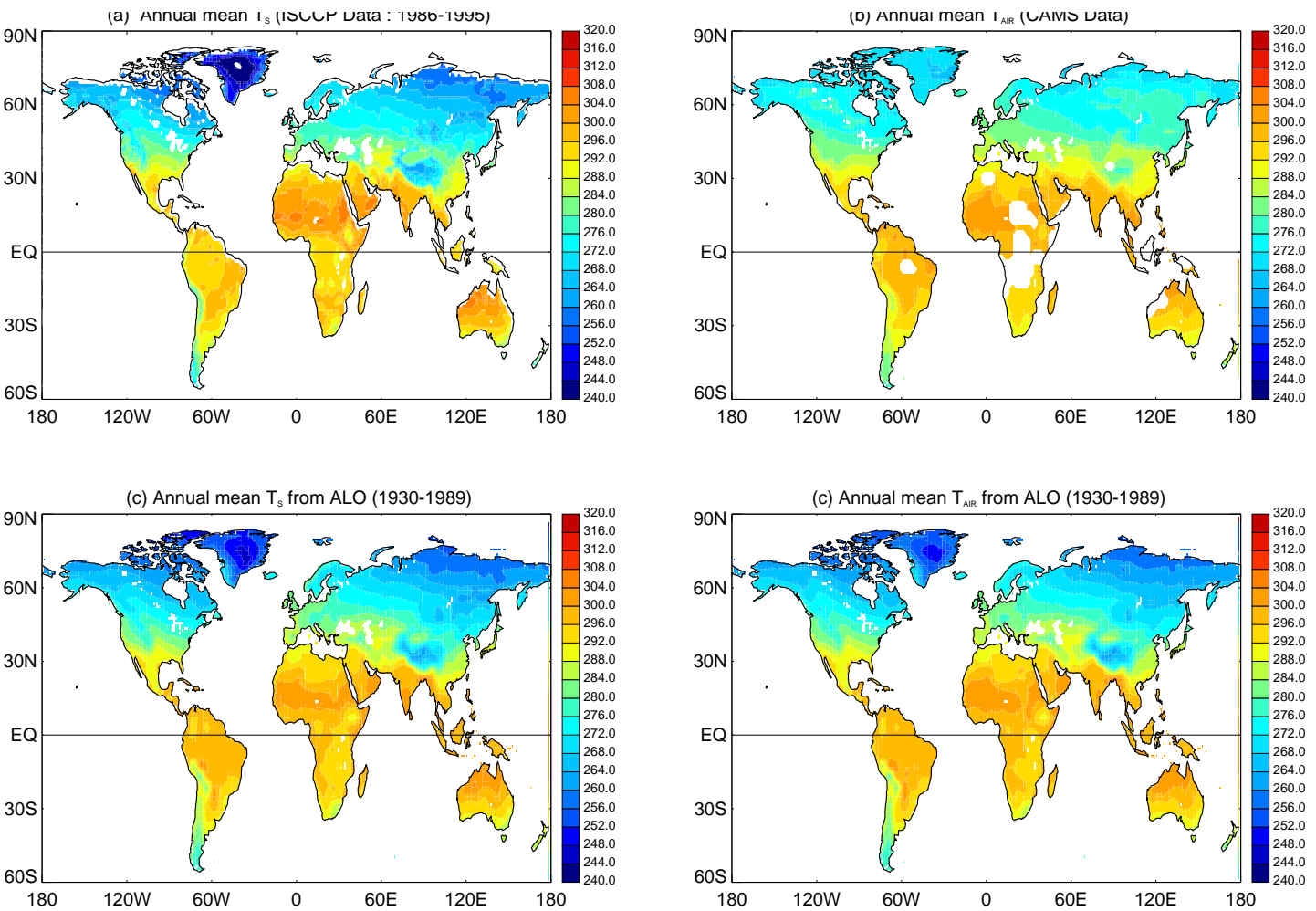


Figure 2: (top left) Annual mean clear-sky skin temperature calculated from the ISCCP (1986-1995) data, (top right) Annual mean T_{air} from CAM5 data, (bottom left) Annual mean surface temperature from the ensemble ALO, and (bottom right) Annual mean T_{air} from the ensemble ALO. For the CAM5 plot, whited-out areas indicate a lack of data. Units are [K].

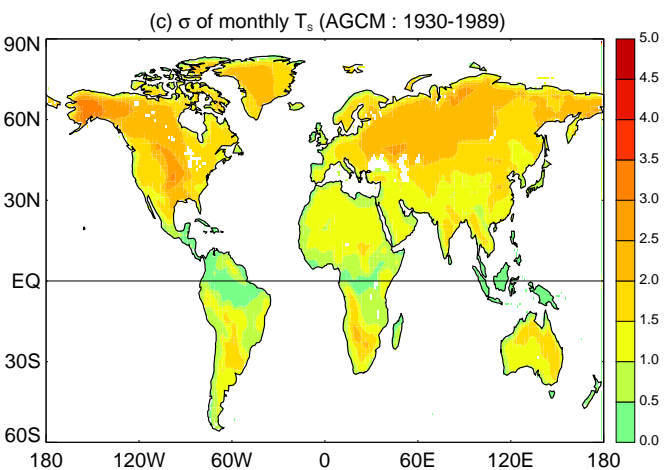
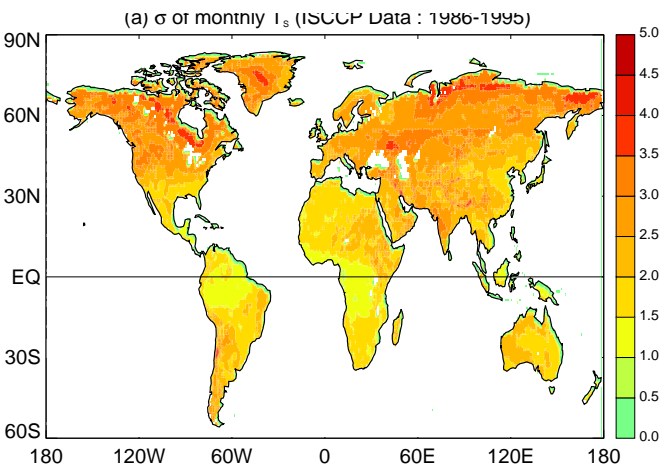
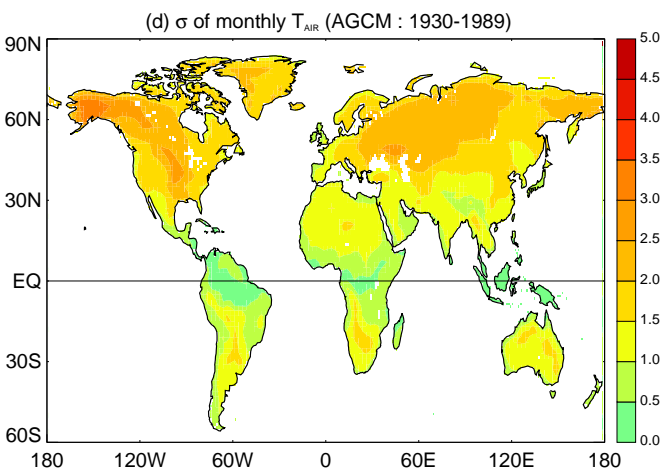
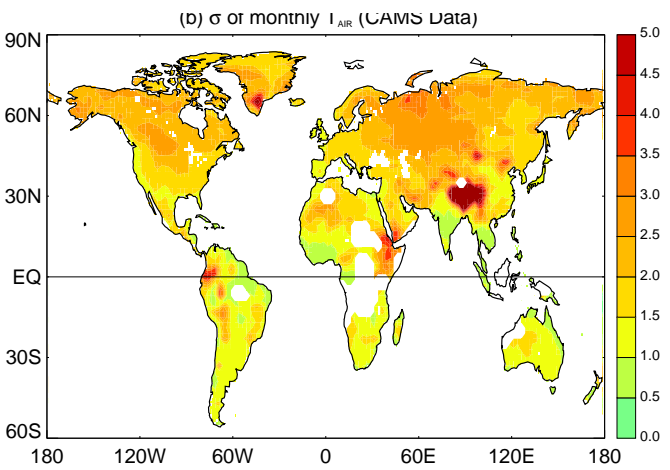


Figure 3: Standard deviations of monthly: (top left) skin temperature calculated for the ISCCP (1986-1995) data, (top right) T_{air} from CAMS data, (bottom left) surface temperature from the ensemble ALO, and (bottom right) T_{air} from the ensemble ALO. For the CAMS plot, whited-out areas indicate a lack of data. Units are [K]

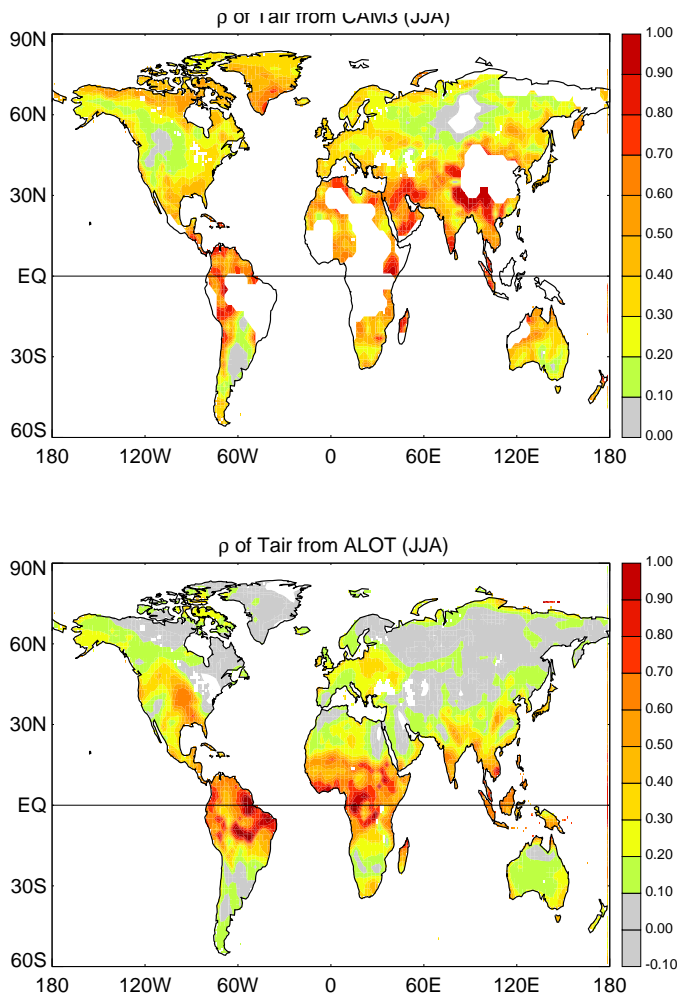
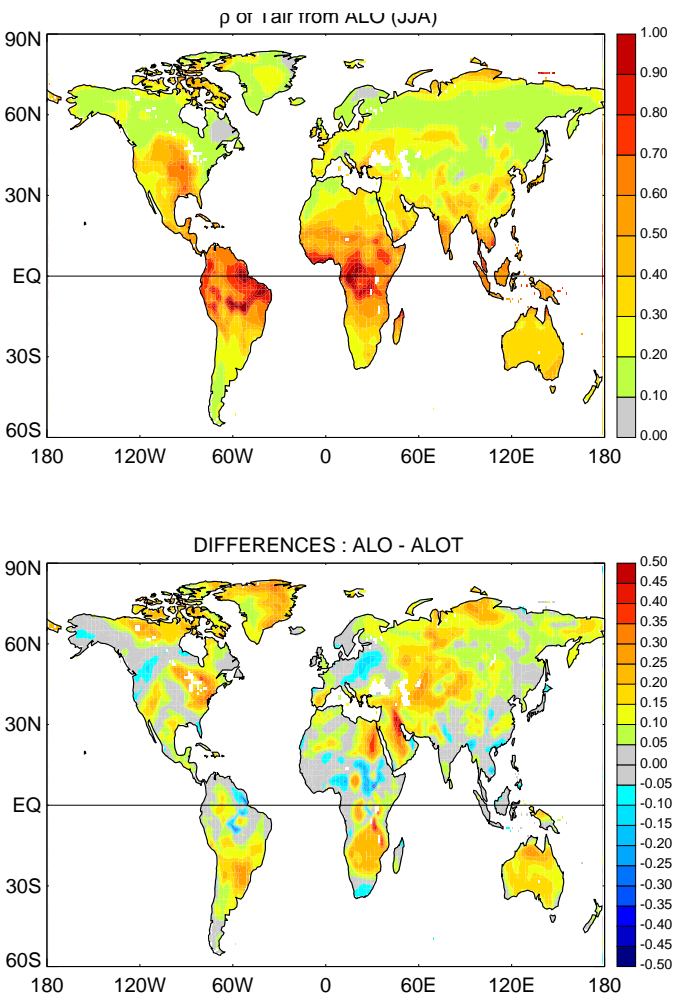
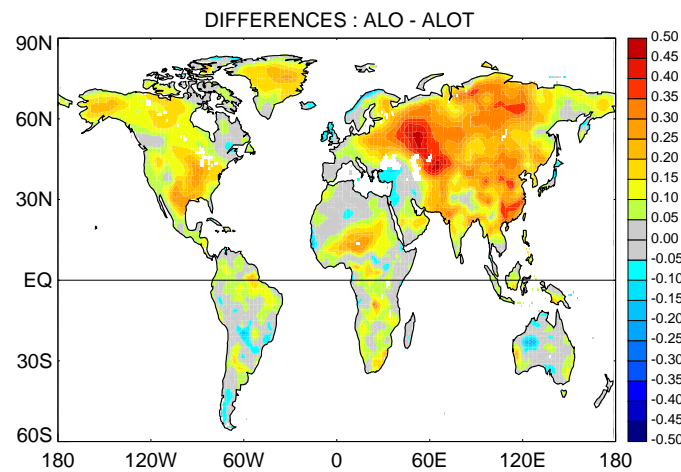
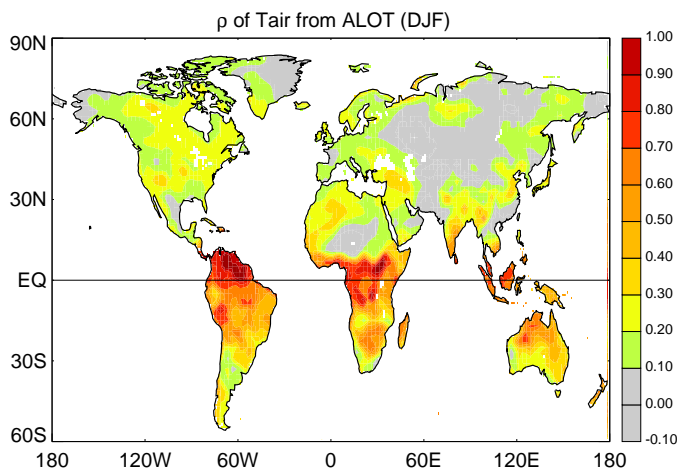
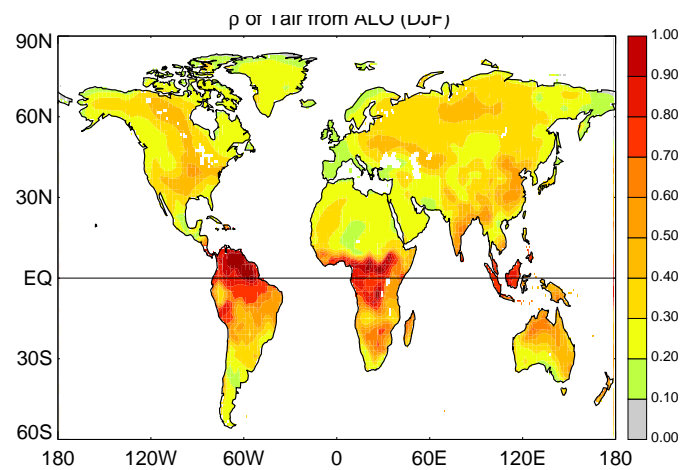
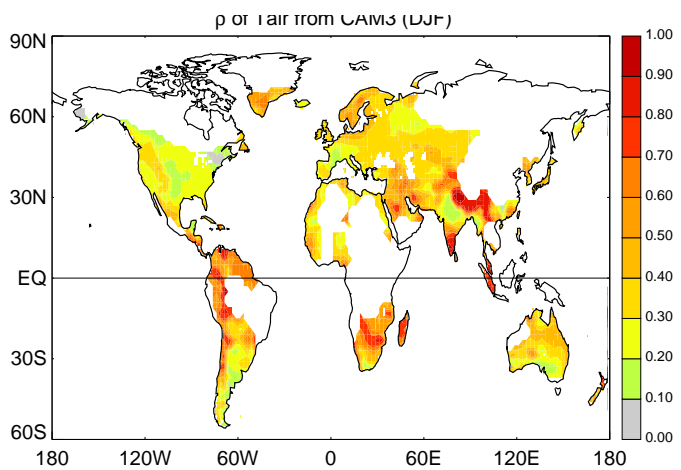


Figure 4: One-month-lagged autocorrelation of Tair (ρ) for boreal summer (JJA): (top left) from CAMS, (top right) from the ensemble ALO, (bottom left) from the ensemble ALOT. (bottom right) Differences ALO – ALOT. For the CAMS plot, whitened-out areas indicate a lack of data.

Figure 5: Same as Figure 4, but for the winter (DJF).



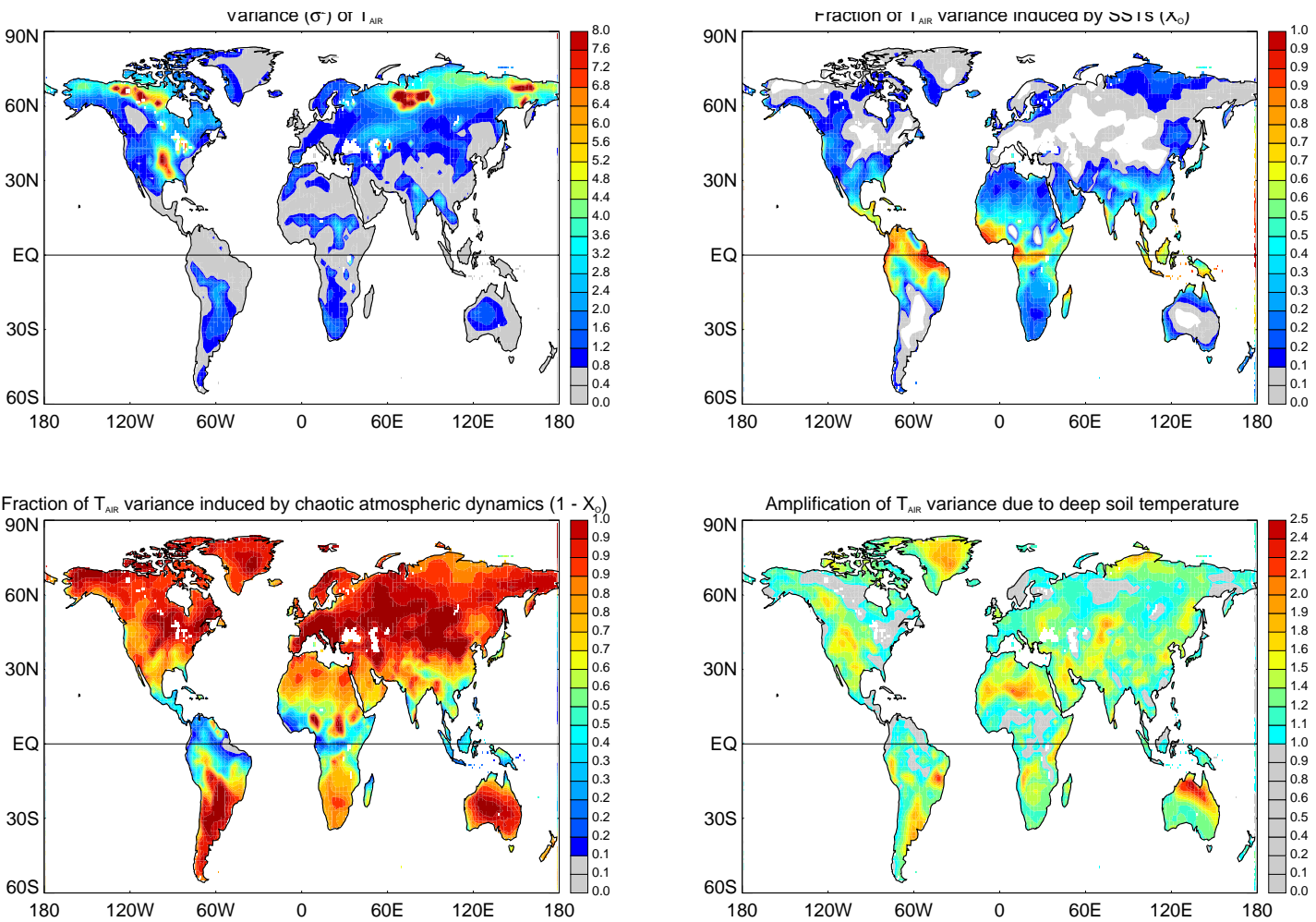
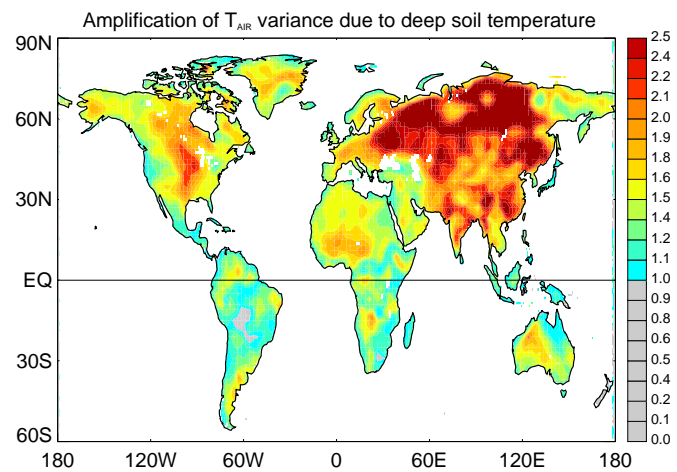
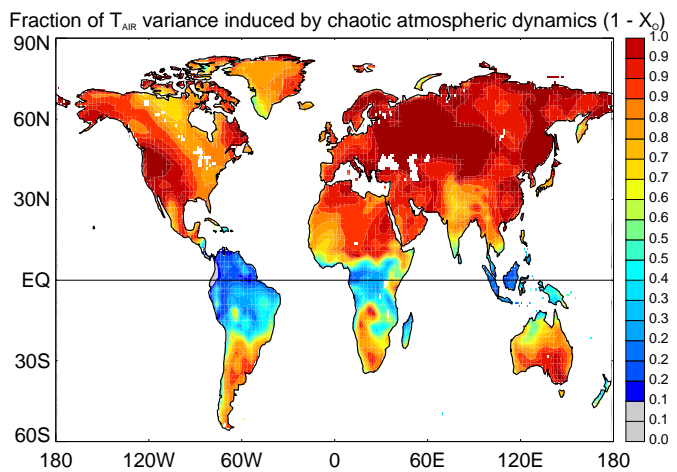
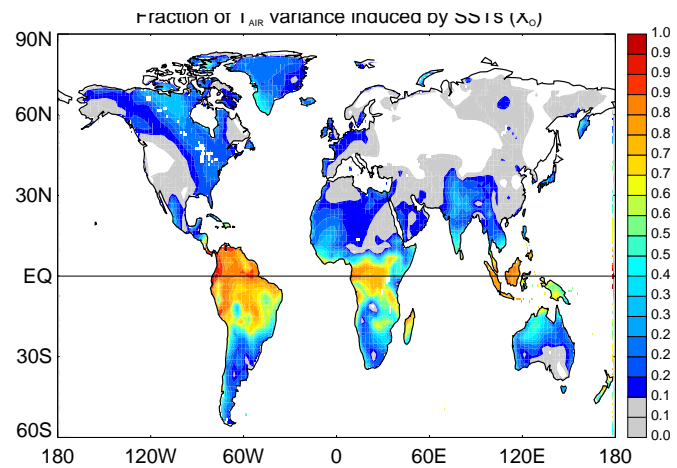
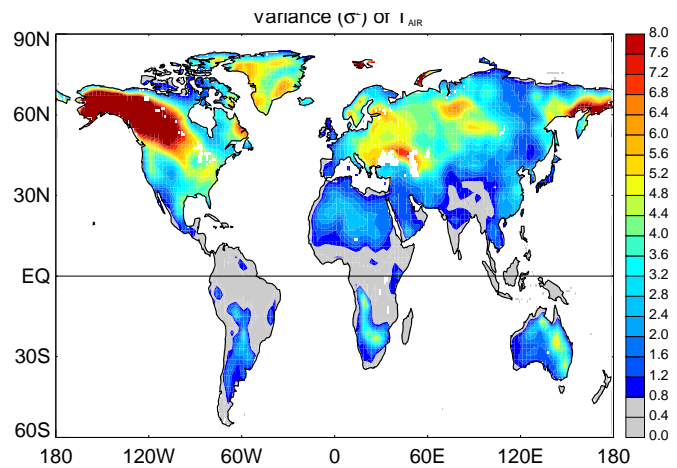


Figure 6: Breakdown of the contributions of oceanic, atmospheric, and deep soil temperature variance to T_{AIR} variance, assuming a linear framework for the boreal summer (JJA). Top left: T_{AIR} variance from ALOT [K^2]. Top right: The fraction of the T_{AIR} variance induced by variable SSTs [XO from Eq. 3]. Bottom left: The fraction of the T_{AIR} variance induced by chaotic atmospheric dynamics ($1 - XO$). Bottom right: Amplification of variance due to deep soil temperature variance ($\frac{\sigma_{\text{ALOT}}^2}{\sigma_{\text{ALOT}}^2}$ for T_{AIR}).

Figure 7: Same as Figure 6, but for the winter months (DJF).



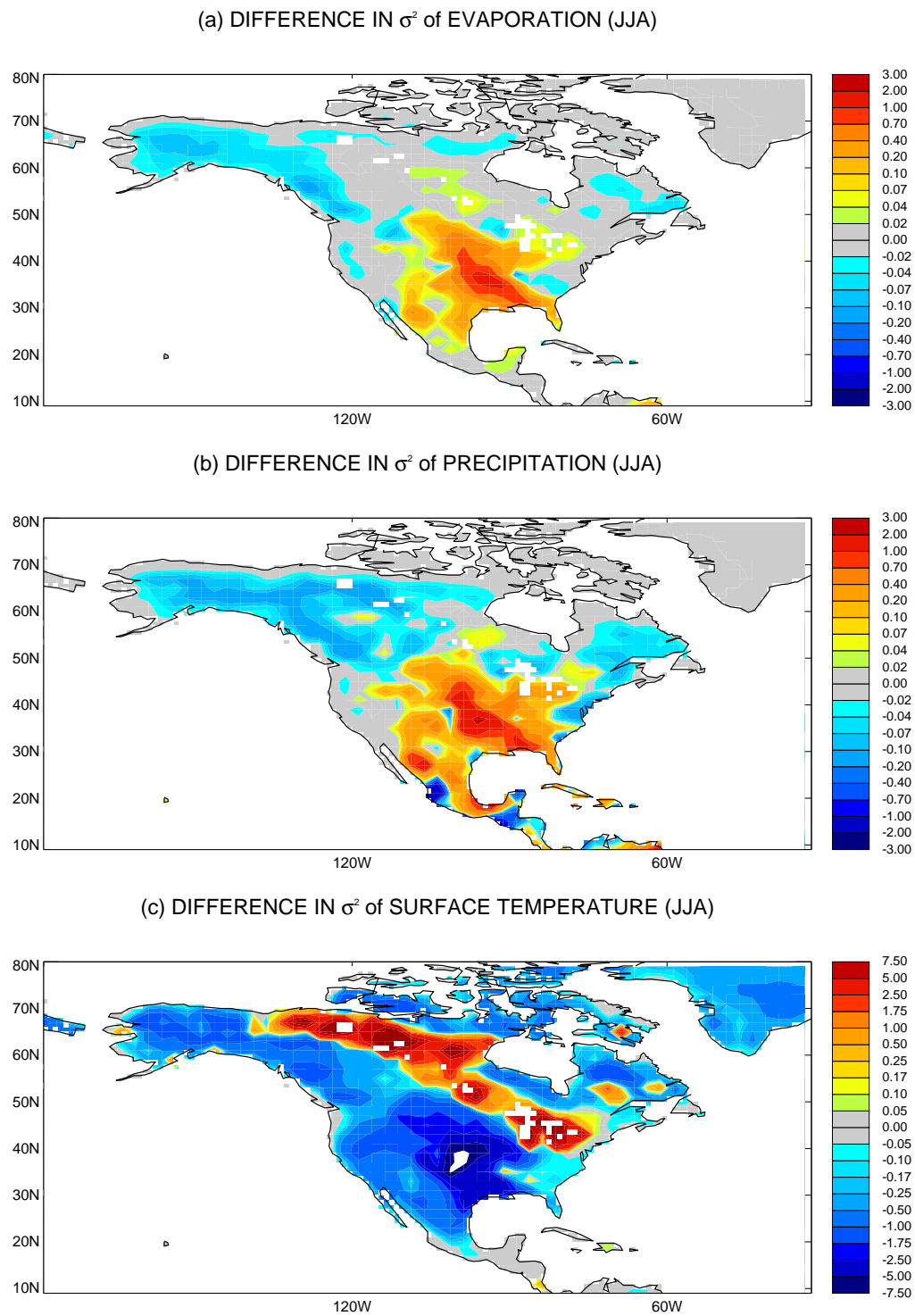


Figure 8: ALO and ALOT Comparison (ALOT – ALO) : (a) Difference in variance (σ^2) of evaporation for boreal summer (JJA) [mm^2d^{-1}], (b) same but for precipitation [mm^2d^{-1}], and (c) same but for surface temperature [K^2].

Experiment identifier	No. of Simulations in ensemble	Length of each simulation	Total years	Experiment description
ALO	10	70	700	Interactive land, Interannually varying ocean
ALOT	1	60	60	Interactive land, Interannually varying ocean, prescribed daily deep soil temperature climatology
AL	1	200	200	Interactive land, climatological ocean

Table 1: Summary of experiments performed.